communications biology

A Nature Portfolio journal

Article

https://doi.org/10.1038/s42003-025-07751-3

Thrombin cleaves membrane-bound endoglin potentially contributing to the heterogeneity of circulating endoglin in preeclampsia

Divina El Hamaoui[1], Aurore Marchelli[1], Sophie Gandrille[1,2], Etienne Reboul[1], Alain Stepanian[3], Bruno Palmier[1], Luca Jovine[4], Franck Lebrin[5,6], David M. Smadja[1,2], Carmelo Bernabeu[7], Cecile V. Denis[8], Pascale Gaussem[1,2], Samuela Pasquali[9], Alexandre Kauskot[8] & Elisa Rossi[1]

Increased levels of soluble endoglin (sEng) are found in serum, plasma, and urine of preeclampsia patients. sEng is released from membrane-bound endoglin through the proteolytic activity of metalloproteases, but its structural heterogeneity suggests the involvement of additional proteases. Considering the roles of thrombin and sEng in preeclampsia pathogenesis, we investigated whether thrombin cleaves endoglin. Sequence analysis revealed a conserved peptide in endoglin similar to the α-thrombin cleavage site of protease-activated receptor-1. Western blot analysis of plasma from preeclamptic women showed endoglin fragments consistent with thrombin-mediated cleavage. Incubation of purified endoglin with thrombin generated specific fragments, whose N- and C-terminal sequencing confirmed the predicted cleavage sites. Furthermore, thrombin treatment of endoglin-expressing cells released sEng and reduced cell surface endoglin. These findings suggest that multiple protease-targeted cleavage sites lead to the generation of sEng fragments, which may reflect endothelial dysfunction and preeclampsia progression.

Endoglin, also named CD105, is known to be an auxiliary receptor for the transforming growth factor β (TGF-β) family including Bone Morphogenetic Protein 9/10 (BMP9/10), which plays important roles in vascular physiology, angiogenesis and vascular remodeling[1] and adhesion[2,3]. Mutations in the human endoglin gene (*ENG*) are responsible for hereditary hemorrhagic telangiectasia (HHT) type 1 (HHT1). HHT is a rare vascular disorder characterized by angiodysplasias ranging from large Arteriovenous Malformations (AVMs) in internal organs to small mucocutaneous telangiectases. HHT affects 1 in 5000 to 10,000 people worldwide[4]. Endoglin (Eng) is mainly expressed on endothelial cells[5], endothelial progenitor cells[3], mesenchymal stromal cells (MSCs)[6] and syncytiotrophoblasts of the neonatal placenta[7].

Membrane Eng is a homodimer of approximately 180 kDa, whose monomers are linked by intermolecular disulfide bonds[8]. It contains: i) an orphan N-terminal region (OR; amino acids 26–337), involved in the binding of its ligands, namely BMP9 and BMP10[9]; ii) a bipartite C-terminal zona pellucida (ZP) module (amino acids 338–581)[10] involved in integrin-mediated cell adhesion[11]; iii) a single transmembrane domain (amino acids 587–611); and iv) a short cytoplasmic peptide (amino acids 612–658)[12].

As recently reviewed[11,13], several studies have reported increased expression of circulating forms of endoglin in serum, plasma, or other body fluids in patients with cancer and other pathological conditions. This form, called soluble endoglin (sEng), consists of the ectodomain of Eng, and has been postulated to be cleaved by the action of metalloproteases, mainly matrix metalloprotease 14 (MMP14)[14,15]. In fact, an 80–75 kDa sEng results from the cleavage of Eng by MMP14 at the endothelial cells (ECs) surface; the cleavage site is shown at position 586, leading to the release of the full-length

[1]Innovative Therapies in Hemostasis, INSERM U1140, Université Paris Cité, Paris, France. [2]Service d'hématologie biologique, AP-HP, Hôpital Européen Georges Pompidou, F-75015 Paris, France. [3]Service d'Hématologie biologique, Hôpital Saint-Eloi - 80 avenue Augustin Fliche – F-34090, Montpellier, France. [4]Karolinska Institutet, Department of Medicine (MedH), Blickagången 16, SE-141 83 Huddinge, Sweden. [5]Einthoven Laboratory for Experimental Vascular Medicine, Department of Internal Medicine (Nephrology), Leiden University Medical Center, Leiden, The Netherlands. [6]Institute Physics for Medicine Paris, INSERM U1273, ESPCI Paris-PSL, CNRS UMR8063, F-75015 Paris, France. [7]Centro de Investigaciones Biológicas Margarita Salas, Consejo Superior de Investigaciones Científicas (CSIC), 28040 Madrid, Spain. [8]HITh, Unite Mixte de Recherche 1176 INSERM, Université Paris-Saclay, Le Kremlin-Bicêtre, France. [9]Laboratoire Biologie Fonctionnelle et Adaptative, INSERM ERL1133 F-75013, Paris, France. e-mail: elisa.rossi@u-paris.fr

ectodomain (amino acids 26–586)[15]. sEng has been described to be released from the placenta into the maternal serum of women with proclamation (PE) and increases with disease severity[16]. Supporting this view, sEng, individually or in cooperation with the placental soluble fms-like tyrosine kinase 1 (sFlt1), induces endothelial dysfunction, vascular permeability and hypertension in vivo[11,13]. Purified sEng from PE women serum showed a band at 65–60 kDa on electrophoresis[7]. The evidence of different lengths of sEng (at least 80–75 and 65–60 kDa) observed in serum strengthens the hypothesis that there are several cleavage sites leading to different sEng sizes[7,16]. Mass spectrometric analysis of endoglin purified from PE patient serum (65 kDa band) revealed that sEng extends at least to arginine 406; however, neither the C-terminal residue nor the corresponding proteolytic enzyme acting on sEng was identified[16]. Importantly, identification of sEng in those studies was performed using the monoclonal antibody P4A4, whose epitope is located within the 54 amino acid region of endoglin from Y277 to G331. As a result, one could speculate that there may be other forms of sEng outside the range covered by the P4A4 antibody. Furthermore, sEng expressed in mammalian cells was shown to be a mixture of dimers and monomers[17], but no explanation was provided for the generation of monomeric or shorter sEng. Thus, the existent heterogeneity of sEng lengths[7] and the circulation of monomeric sEng in PE[17] remains a puzzle to be untangled.

In 2005, Tang and colleagues proposed that thrombin induces endocytosis of endoglin and type II TGF-β receptors and downregulation of TGF-β signaling in EC[18], but this study did not provide information or evidence regarding the mechanism of endocytosis or the possible release of sEng from the cell surface. Thrombin (Thr) is a potent vascular physiological agonist belonging to the trypsin family of serine proteases with multifunctional effects and key roles in hemostasis and thrombosis[19]. Besides its procoagulant function in the production of fibrin, Thr regulates multiple cellular processes by cleaving the protease-activated receptors 1 and 4 (PAR-1 and PAR-4) in platelets, leukocytes, ECs and vascular smooth muscle cells[20]. Interestingly, it was demonstrated that: i) elevated levels of Thr production have been correlated to the underlying causes of PE; and ii) women suffering of PE exhibit an excessive generation of Thr[21,22]. Thus, given that Thr and sEng have been proposed to be involved in the pathogenesis of PE, this led us to investigate whether Thr is able to cleave Eng.

In this work, we provide evidence for the first time that Thr cleaves membrane and soluble forms of endoglin. This pathway could reflect the endothelial dysfunction during PE and might be involved in the progression of PE disease.

Results

Plasma and Serum Levels of sEng in preeclampsia (PE)

Plasma and serum levels of sEng were measured in 60 subjects, including 20 non-pregnant controls, 20 pregnant controls and 20 PE patients. sEng concentration (ng/mL) in both plasma and serum was significantly higher in PE than in control plasma [57.35 ± 18.2 (PE) *versus* 3.47 ± 0.68 (non-pregnant controls) or 7.05 ± 1.83 (pregnant controls) ng/ml], and control serum [47.90 ± 24.50 (PE) *versus* 3.70 ± 0.77 (non-pregnant controls) or 7.74 ± 1.95 (pregnant controls) ng/mL] (Fig. 1a, b). Plasma and serum

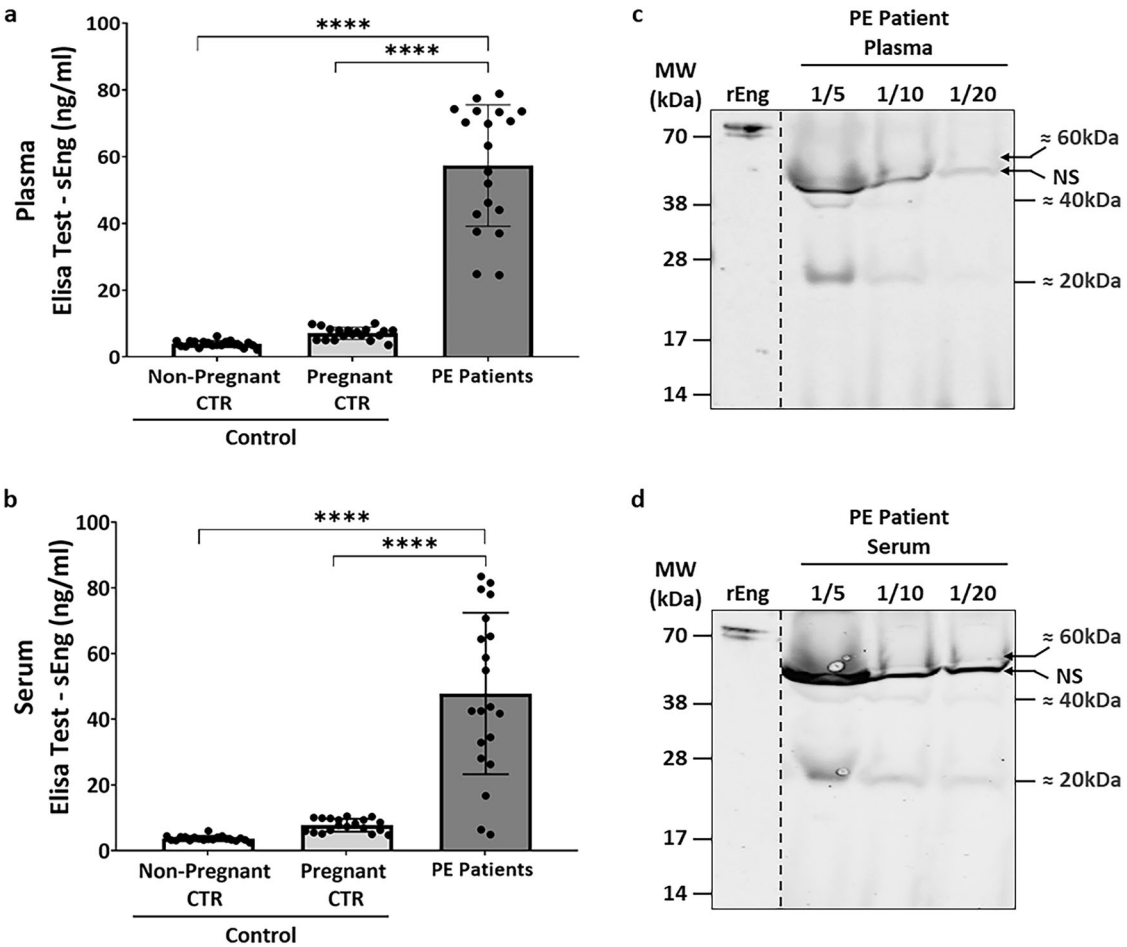

Fig. 1 | Plasma and serum analysis of patients with preeclampsia. The levels of sEng in (**a**) plasma and in (**b**) serum were quantified using an ELISA kit assay in a cohort of 60 patients. This cohort comprised 20 non-pregnant women controls, 20 pregnant women controls, and 20 cases diagnosed with preeclampsia. **c** Plasma and (**d**) serum samples from preeclampsia patients diluted to ratios of 1:5, 1:10, or 1:20 and reduced with DDT, were subjected to analysis through SDS-PAGE and Western blot with Endoglin/CD105 polyclonal rabbit antibody (ProteinTech). rEng at 100 ng/mL was used as control. The data is presented as mean ± S.D. Statistical significance was determined at $^{*}P < 0.05$, $^{**}P < 0.01$, $^{***}P < 0.001$, and $^{****}P < 0.0001$. NS indicates a non-specific band.

Fig. 2 | Predictive study to identify possible cleavage motifs. a Possible cleavage motifs found by the Profile Specific Scoring Matrix analysis (left column) and their associated score (right column) combined with accessibility (A: highly accessible; PA: partially accessible; B: buried) giving the extent to which each sequence corresponds to the profile extracted from known thrombin cleavage motifs. The scale of the score is arbitrary and the sequences highlighted in bold have significantly higher scores (score > 6) than the others and are accessible on the surface of Eng within the context of its open homodimeric structure. Colored sequences correspond to those later determined experimentally as cleavage sites. **b** Theoretical model of endoglin showing possible thrombin cleavage sites which corresponds to location of the experimentally determined cleavage sites on the structure of the open Eng. **c** The top panel shows a theoretical model of thrombin (blue) in complex with the CGGRLQTS sequence of endoglin, obtained by docking. A detailed view of the corresponding putative interaction site is shown in the bottom panel ("zoom").

a

Sequence	score	accessibility	position from ETVHC
GPERGEVT	5.49	A	13
TWPREVLL	**11.52**	**A**	**67**
AAERGPIT	3.75	A	127
ILLRLGQA	-3.33	B	145
DMGRTLEW	8.65	B	166
LEWRPRTP	6.99	PA	171
WRPRTPAL	**11.43**	**PA**	**173**
ALVRGCHL	5.1	PA	179
HILRVLPG	1.69	B	196
AGPRTVTV	**10.25**	**PA**	**206**
KNIRGFKL	8.06	A	262
GEARMLNA	1.49	PA	278
CGGRLQTS	3.55	A	307
AEDRGDKF	3.14	A	373
FVLRSAYS	6.67	A	380
SPQRKKVH	-0.29	A	411
VQVRVSPS	2.56	B	452
IQGRAAKG	5.48	A	484
GDPRFSFL	11.24	B	503
VALRPKTG	-1.51	PA	528
EVHRTVFM	10.32	PA	540
VFMRLNII	1.83	PA	545

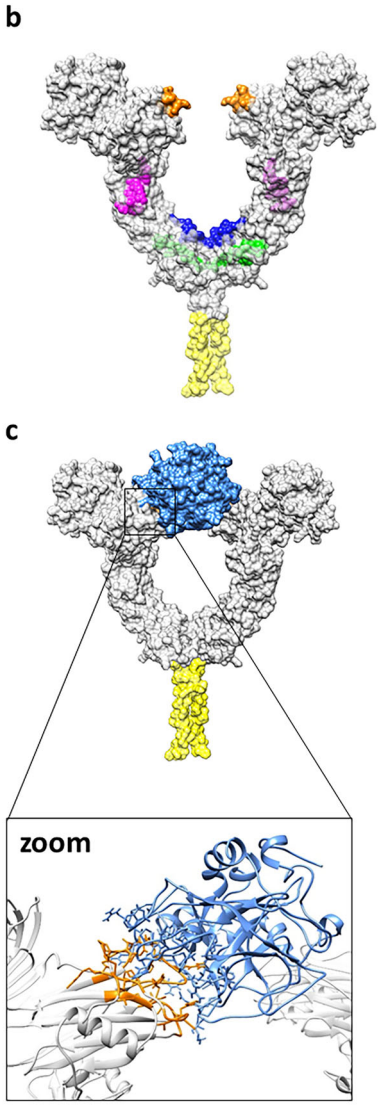

analyzed by WB for Eng showed different molecular weight bands of sEng: 60, 40 and 20 kDa (Fig. 1c, d; Supplementary Fig. 1a–c). The visualization of these bands was possible thanks to a new antibody against endoglin that targets over 50% of the Eng sequence (residues 331–658) (Proteintech, #10862-1-AP), at variance with the P4A4 antibody that only targets ~10% of the sequence (residues 270-330) (Supplementary Fig. 2). These previously undescribed Eng fragments suggested the existence of novel cleavage sites in the endoglin sequence.

Computational analysis revealed potential Thr cleavage sites in endoglin

When searching for potential new cleavage sites, amino acid sequence analysis of endoglin highlighted the presence of a GD**PRFSFLL**H sequence (residues 526–534). Of note, a clear similarity was found (in bold) to the protease activated receptor PAR-1 site PRSFLL, a sequence known to be cleaved by Thr[23], a protease involved in PE[21,22]. Alignment of the human endoglin amino acid sequence with those of 10 other mammal species revealed that this sequence (amino acids 528 to 534) is highly conserved among different species (Supplementary Fig. 3a, b), potentially suggesting that this may be an important recognition site for a putative protease. Given the high sequence similarity to the Thr cleavage site of PAR1, we hypothesized that Thr might also be able to cleave endoglin. The crystal structure of the ZP module of ENG[24] shows that the GD**PRFSFLL**H sequence is not highly exposed within the context of the ZP-C module and is thus unlikely to be readily accessible to Thr or other proteases. However, it could become accessible upon structural rearrangements of ENG, possibly triggered by prior cleavage at other sites. Indeed, a Profile Specific Scoring Matrix analysis identified several other potential cleavage sites with relatively high scores and accessibility (Fig. 2a–c). As a proof of principle, computational docking of Thr to the site 329-CGGRLQTS-338 (Fig. 2c, bottom panel) suggests that the latter may be cleaved by the protease. Looking at the crystal structure of ENG, this site appears to be the most exposed to the solvent, and it could be a plausible first target for the protease, since it is easily accessible. This docking result is not meant to be a proper model for a Thr and ENG complex, but just a simulation supporting its existence. These analyses suggest that 1) several possible cleavage sites are present on the ENG sequence, 2) the approach of Thr to at least one of the identified cleavage sites is plausible. These results encouraged a further experimental exploration for cleavage of fragments of different sizes (Fig. 2a, b).

Thrombin cleaves endoglin in vitro and generates different fragments

To address the above hypothesis, we investigated whether Thr can target Eng in vitro. Physiologic concentrations of free Thr generated during coagulation are estimated to vary from 1 nM to over 500 nM[25,26], whereas pathological concentrations can reach up to 10 μM[27]. Thus, we tested the

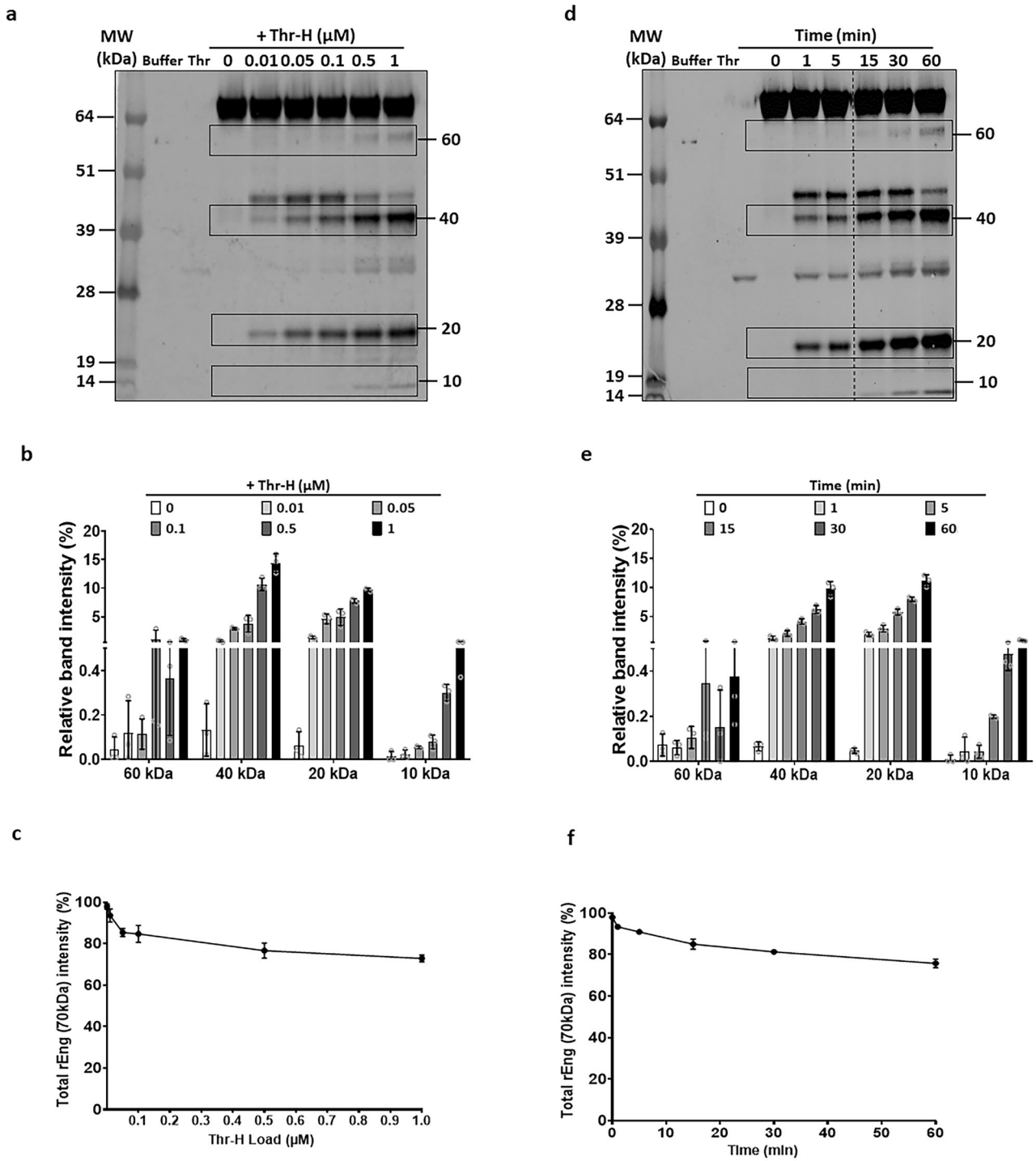

Fig. 3 | Dose and time dependent cleavage of human rEng by thrombin. rEng at a concentration of 20 μg/mL was treated at 37 °C **a** with increasing concentrations of Thr-H : 0, 0.01, 0.05, 0.1, 0.5, or 1 μM for 1 h. Following treatment, the samples were resolved using SDS-PAGE and subsequently analyzed by Western blotting with Endoglin/CD105 polyclonal rabbit antibody (ProteinTech). **b** The percentage of all cleaved bands obtained in **a** by the action of Thr-H on Eng was quantified relatively to the total rEng (70 kDa). **c** Percentage of the 70 kDa band reduction, specific to the total rEng band from **a**. **d** The same procedure described in **a** was repeated (Eng 20 μg/mL, treatment at 37 °C), but using a fixed concentration of 1 μM of Thr-H for varying durations: 0, 1, 5, 15, 30 or 60 min. **e** Graph of percentage of all cleaved bands resulting from the action of Thr-H on rEng at various time intervals. **f** Percentage of the 70 kDa band reduction, specific to the total rEng band from **d**. left. In **a** and **d** the band above 40 kDa (of approximately 50 kDa) was not reproducibly observed in the repeated experiments and was not further studied. The data is presented as mean ± S.D. from three conducted experiments. All images analysis were performed using Image Studio™ Lite software. The dashed line in panel **d** indicates a cut made in the gel where a blank column had been.

ability of α-thrombin (Thr-H) to cleave rEng within this concentration range (10 nM-1 μM) during 1 h of treatment. Using a polyclonal antibody against Endoglin, we detected different rEng cleavage products (Fig. 3a). Indeed, bands at ≈60, 40, 20 and 10 kDa were detected in a Thr-H concentration-dependent manner (Fig. 3a, b) simultaneously with a decrease of the total rEng (non-cleaved, 70 kDa) (Fig. 3a–c). All bands were detectable from the lowest concentration of Thr-H (10 nM). Of note, in the absence of Thr-H no cleavage of rEng was observed after 1 h of incubation at 37 °C. A kinetic study performed at a concentration of 1 μM of Thr-H (from 1 min to 1 h) revealed that the bands appeared already at 1 min and progressively

increased up to 1 h of treatment (Fig. 3d, e). Conversely, a progressive decrease of the total endoglin was observed (Fig. 3d–f). The smallest fragment (10 kDa) was the last one to be detected and appeared after 15 min (Fig. 3e). Of note, upon thrombin treatment, a band above 40 kDa (of approximately 50 kDa) was observed in some experiments (see for example Fig. 3a, d). However, depending on the commercial batch of the rEng, the intensity of this band was not always reproduced in the repeated experiments, likely due to changes in its glycosylation pattern. For this reason, the band above 40 kDa was not further studied. Kinetic- and Thr-H concentration-dependence of the generation of small bands (40, 20 and 10 kDa) was confirmed in a Simple Western (WES) assay (Supplementary Fig. 4a). Moreover, a similar pattern was detected by Western blot at a lower Thr-H concentration (0.1 μM), with all bands appearing as early as 1 minute after Thr-H treatment (Supplementary Fig. 5a, b). Of note, β-thrombin (Thr-C) cleaved rEng in fragments of similar molecular weights as α-thrombin (Thr-H), and a supplemental smaller band at around 2 kDa was observed for both Thr (Supplementary Fig. 4b). Altogether, our data demonstrate that Thr (both α- and β-thrombin) cleaves Eng in vitro to generate different Eng fragments in a time- and concentration-dependent manner.

Identification of the endoglin sequences cleaved by thrombin

We then investigated Thr cleavage sites in rEng by sequencing each fragment. To this end, we fixed the experimental conditions: 1 μM of Thr-H, during 1 h at 37 °C, followed by detection and isolation of each fragment from Coomassie blue-stained gels and their N- and C-terminal (N-t and N-c, respectively) amino acid sequencing (Fig. 4a, Supplementary Fig. 6), By Coomassie blue staining of SDS-PAGE gels, we identified all the bands detected by WB (60, 40, 20 and 10 kDa) as well as an extra band at 8 kDa (Fig. 4a, Supplementary Fig. 6). In agreement with our previous data (Fig. 2), we observed a significant 50% decrease of the total rEng (70 kDa) upon Thr digestion (Fig. 4b). The most abundant fragments were the bands of 40 kDa and 20 kDa (Fig. 4c). As a preliminary control, we analyzed the sequence of the initial rEng used in the study. According to N-t sequence analysis, the primary structure of recombinant mature Endoglin of 70 kDa starts at Glu 26 (**ETVHC**) and ends in Gly 586 (**CTSKG**), as expected from the commercial datasheet provided by the manufacturer and similar to the described cleavage produced by MMP14[7,15].

N-t analysis demonstrated that both the 60 kDa and 40 kDa fragments start with **ETVHC** (Fig. 4d, e; Supplementary Fig. 7a), but C-t analysis was not able to identify with precision the corresponding C-terminal (Fig. 4d, e). However, immunoblot with the monoclonal antibody MAB1097 (Supplementary Fig. 5c) that specifically recognizes the endoglin orphan region (Supplementary Fig. 2) suggests that the 40 kDa fragment ends with CGGR (Figs. 2 and 4), as also supported by predictive studies (Fig. 2a, b). Interestingly, this cleavage site (GGRLQT) maps within the 18-residue linker between the OR and the ZP module[10], and it can be hypothesized that this precise location, right in the boundary between those two different functional regions, has a potentially relevant biological role. Considering the fragment of 20 kDa, N-t starts with **SAYSS** (Ser 407) (Fig. 4d–f; Supplementary Fig. 7b), whereas the C-t ends with the fragment corresponding to CTSKG (Gly 586) (Fig. 4d–f). Of note, the N-t cleavage site for the 20 kDa fragment, between residues 406 and 407, is exactly the last residue previously mapped in sEng purified from PE patients' plasma[16]. The 10 kDa fragment presents the N-t starting with **AAKGN** (Ala 511) (Fig. 4d–f; Supplementary Fig. 7c) and the C-t ends with the peptide corresponding to CTSKG (Gly 586) (Fig. 4d–f). The N-t starting sequence of 20 kDa and 10 kDa fragments confirmed the prediction of Thr cleavage suggested by modelling (Fig. 2). The fragment of 8 kDa (Fig. 4a, c) was also analyzed by N-t analysis and starts with **SFLLH** (Ser 531) (Fig. 4d–f; Supplementary Fig. 7d), but its C-t was not detectable (Fig. 4d, e). However, by WES we identified the presence of a 2 kDa fragment after incubation (at different times from 1 min to 1 h) with Thr-H (Supplementary Fig. 4a), suggesting that the 10 kDa fragment can be further cleaved, leading to two smaller fragments of 2 and 8 kDa, as predicted in Fig. 2a, b and Fig. 4e, f. This result was also confirmed using Thr-C (Supplementary Fig. 4b).

It can be speculated that after an initial cleavage, the molecule will be open and will become more accesible for further cleavages. Furthermore, the fragment of 40 kDa starting with **ETVHC** also suggests that it can be monomeric because it does not contain Cys residues involved in intermolecular disulfide bonds (Fig. 2a, b; Fig. 4e, f).

By clustal alignment sequence, it is evident that in the mouse endoglin there are different amino acids in the specific cleavage sites predicted in human endoglin (CGGRLQTS, FVLRSAYS, IQGRAAKG), while the sequence FSFLLH is conserved in both species. (Supplementary Fig. 3b). To confirm the specificity of the cleavage in the predicted sequences we treated human and mouse rEng at a concentration of 20 μg/mL with increasing concentrations of thrombin-H (0.01–0.05-0.1-0.5–1 μM) at 37 °C for 1 h. Gels were run simultaneously using MOPS buffer, optimal for revealing the bands at the expected cleavage sites (mutated in mice). Human rEng confirmed the cleavages at 60, 40, and 20 kDa, as expected and showed the uncleaved monomeric form at 75 kDa. The uncleaved murine endoglin appeared as a double band around 95–100 kDa, due to varying levels of glycosylation as informed by the supplier. Consequently, the cleaved bands that may originate from thrombin cleavage at the conserved motif DPRFSFLLH might also appear as a double band with a 5 kDa difference (70–65 kDa). (Supplementary Fig. 5d)

Endoglin is cleaved by thrombin at the cell surface

The above data demonstrate that soluble rEng can be cleaved by Thr. We then investigated the physiological capacity of Thr to cleave endoglin from the cell surface of different cell types expressing surface Eng: ECFCs, HUVECs and MSCs[6,28]. ECFCs were incubated with different concentrations of Thr-H (10 nM, 100 nM, and 1 μM) and HUVECs and MSCs were treated with 1 μM of Thr-H. Importantly, Thr-H treatment did not affect ECFC viability, and cells conserved their monolayer appearance (Fig. 5a–d, Supplementary Fig. 8a). Cellular endoglin cleavage by Thr was analyzed by immunofluorescence. Endoglin-specific fluorescence was reduced in ECFCs after Thr-H treatment compared to control, in a dose-dependent manner (Fig. 5a–c). This result was confirmed with the two other cell types, HUVECs and MSCs, that showed a decrease of endoglin staining on cell surface upon Thr treatment, without any effect on cell viability (Fig. 5d, e). The specificity of Thr cleavage was supported by using the thrombin inhibitor PPACK in assays with ECFC and HUVEC (Supplementary Fig. 8b). Then, we quantified the level of sEng in cell supernatants by ELISA and WES techniques. Interestingly, sEng levels were significantly increased in all cell lines treated with Thr-H compared to controls (Fig. 5f). These results were also replicated with Thr-C. Importantly, the 60, 40 and 20 kDa bands were observed by WES in MSCs and HUVECs supernatants (Supplementary Fig. 8c–f), confirming the results obtained in vitro using rEng. Since the mature cell surface endoglin carries the standard O- and N-glycosylation[8], while rEng which is less glycosylated (R&D, datasheet), the above findings may rule out the possible interference of sEng glycosylation in the Thr cleavage. Supporting this conclusion, endoglin glycosylation occurs in a region of the protein different from those of the Thr cleavage sites (Supplementary Fig. 9). Hence, our data demonstrate that Thr is able to cleave Eng from cell surface, leading to the release in the extracellular medium of different fragments of sEng.

Discussion

Increased plasma sEng levels are an indicator of maternal vascular malperfusion lesions in the placenta of women with PE[29]. PE remains till today a leading cause of maternal and fetal morbidity and mortality. While the pathophysiology of the disease is not yet fully elucidated, it is evident that it revolves around placenta. Cellular ischemia in the preeclamptic placenta creates an imbalance between angiogenic and anti-angiogenic factors in maternal circulation. Eng, a transmembrane co-receptor of TGF-β demonstrating angiogenic effects, is involved in a variety of angiogenesis-dependent diseases with endothelial dysfunction, including PE. Eng expression is up-regulated in preeclamptic placentas, through mechanisms mainly induced by hypoxia, oxidative stress and oxysterol-mediated activation[30].

During the last decade, different sizes of sEng have been described in PE, including the presence of dimeric and monomeric forms in plasma of PE patients[17,31], however so far, no clear explanation for this heterogeneity has been proposed. In non-endothelial cells such as human multiple myeloma cell lines or the mouse myoblast cell line C2C12, both monomeric and dimeric forms of sEng have been reported to inhibit BMP9 signaling when

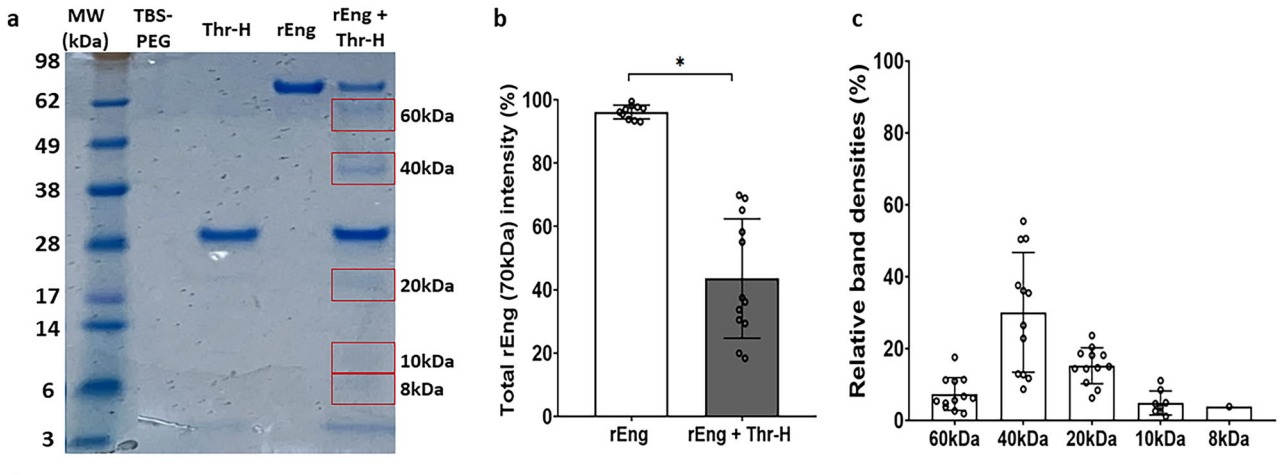

d

Bands	N-Ter	C-Ter	Cleavage position	Cleaved Amino Acid
8kDa	SFLLH	ND	530 - 531	F/S
10kDa	AAKGN	CTSKG	510 - 511	R/A
20kDa	SAYSS	CTSKG	406 - 407	R/S
40kDa	ETVHC	CGGRL ?	329 - 330?	S/C?
60kDa	ETVHC	ND	-	-

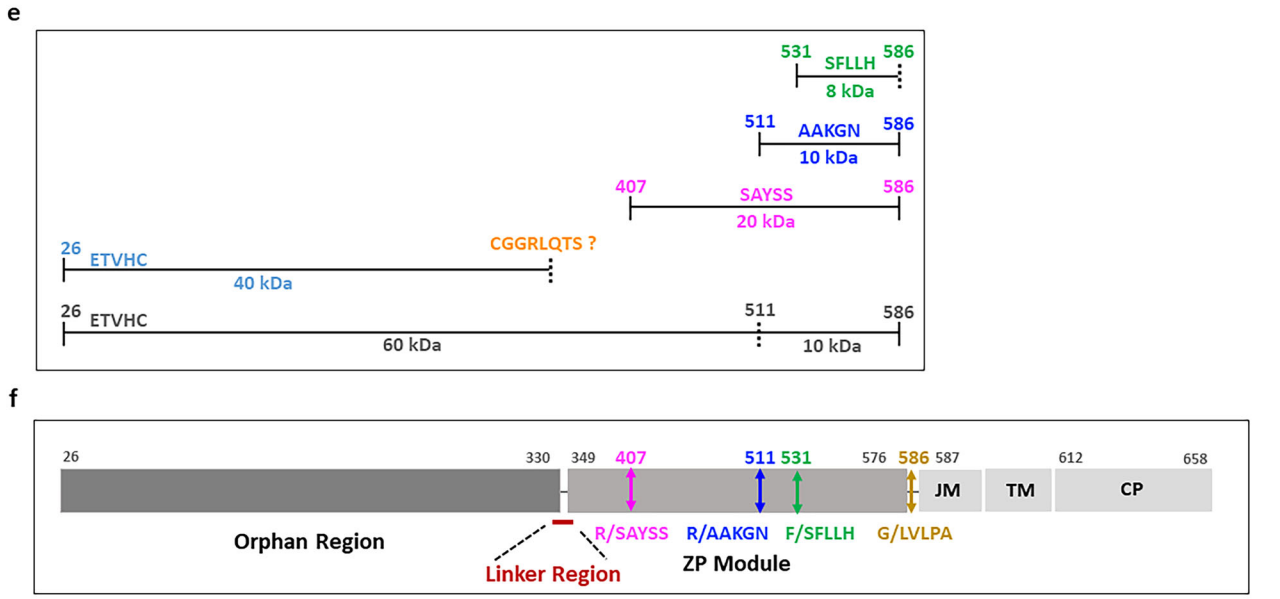

Fig. 4 | Sequencing of thrombin-cleaved endoglin bands. a rEng at a concentration of 20 µg/mL was treated at 37 °C for 1 h with 1 µM of Thr-H. The samples were then resolved by SDS-PAGE and subjected to Coomassie Brilliant Blue staining to identify protein spots for subsequent sequencing. Bands at molecular weights of 60, 40, 20, 10, and 8 kDa were excised, with a minimum of 30 bands at each molecular weight selected for further analysis. Plots showing **b** the decrease in the percentage of the 70 kDa band, specific to the total rEng band and **c** the percentage of all cleaved bands obtained by the action of Thr-H on Eng, quantified relatively to the total rEng (70 kDa). The optical densities of each Coomassie blue-stained protein band were measured using Image Studio™ Lite software. The data is presented as mean ± S.D. from a minimum of 12 conducted experiments. Statistical significance was considered at $^{*}P < 0.05$. **d** Table showing the N-terminal and C-terminal parts of each sequenced band, along with the cleavage position and the cleaved amino acids. The C-terminal information was not determined (ND) for the 8, 40 and 60 kDa bands, and the cleavage position and cleaved amino acids for the last two bands were also unidentified. However, based on the docking data and the Western blot analysis with the monoclonal antibody MAB1097 (R&D), that specifically labels the endoglin orphan region, for we can postulate that the 40 KDa band corresponds to the fragment 329–330. **e** Schematic diagram illustrating the N-terminal cleavage positions and sequences of each band, including known (solid line) and hypothetical (dashed line) C-terminal cleavages. Because the contribution of glycosylation to the molecular weight of each band is unknown, the correlation between molecular weight and primary structure is not to scale. **f** Schematic diagram of mEng, indicating cleavage sites. mEng is composed of an orphan region followed by a juxtamembrane zona pellucida (ZP) module and by transmembrane and short cytoplasmic domains. JM: Juxtamembrane; TM: Transmembrane; CP: Cytoplasmic.

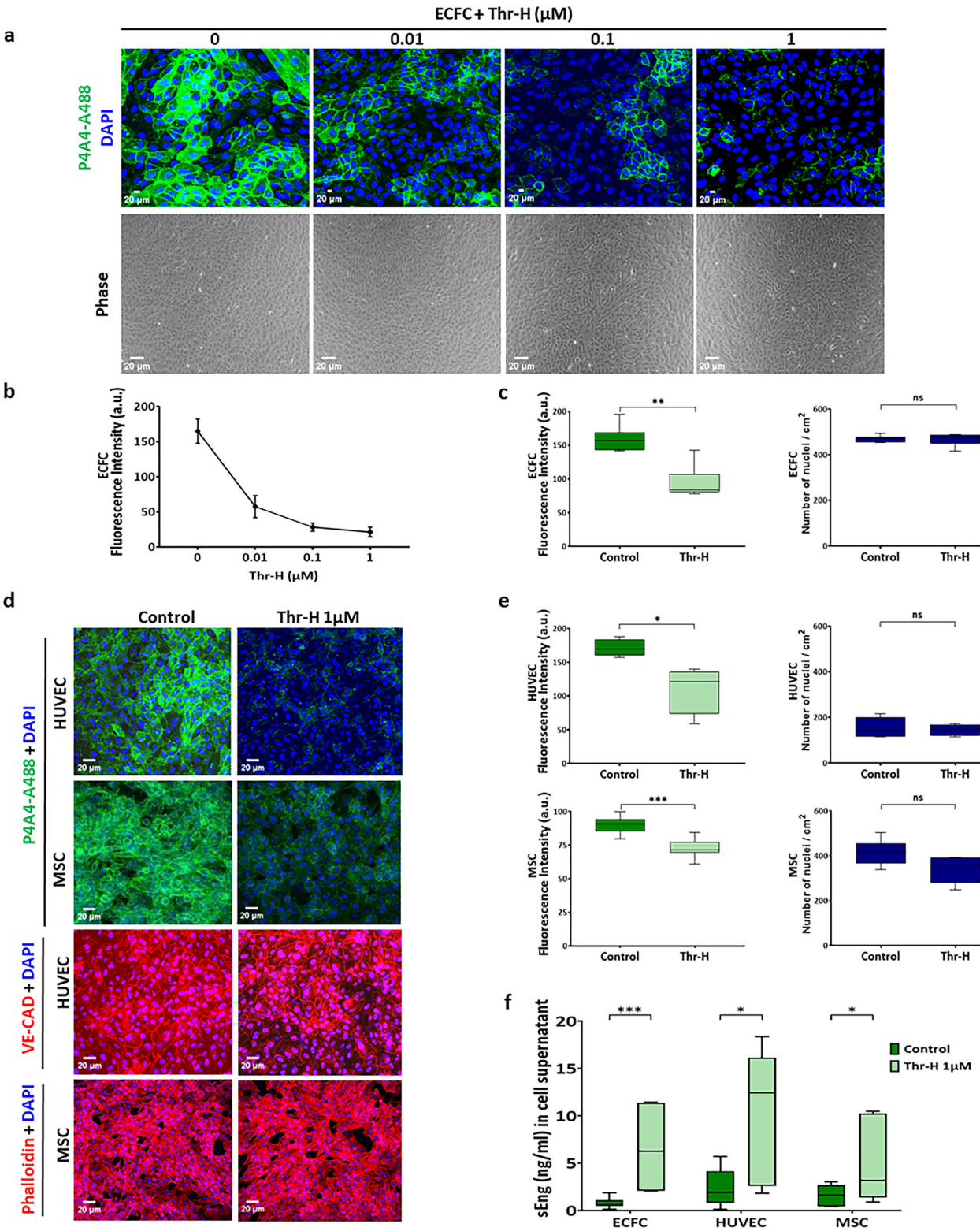

they are present at high concentrations[17]. To date, the only explanation proposed for the production of sEng has been the cleavage produced by metalloproteases that target the GL motif of the juxtamembrane region of endoglin, resulting in a dimeric form of sEng. However, this cleavage alone does not account for the presence of a monomeric form, as the resulting protein would still contain disulphide bridges, leading to a dimeric structure.

The involvement of other metalloproteases, different from MMP14 and MMP12 was investigated without success. For example, MMP15 is localized to the syncytiotrophoblast layer of the placenta, the same site where Eng is expressed. Interestingly, despite being upregulated in PE, MMP15 does not cleave endoglin to produce sEng[32]. Additionally, immunolocalization studies have revealed the presence of MMP16, MMP24 and MMP25 in the syncytiotrophoblast, where Eng is highly expressed. However, these MMPs do not contribute sEng production in pre-eclampsia[33].

It has been postulated that Thr's interaction with the mEng induces Eng internalization. However, this report did not provide details about the

Fig. 5 | In vitro cleavage of cellular Endoglin by thrombin. **a** Immunofluorescence staining of Endoglin was conducted using the Endoglin/CD105 P4A4-Alexa 488 antibody (green) and vectashield mounting medium with DAPI (blue) after treating ECFC with increasing concentrations of Thr-H (0.01, 0.1 and 1 μM). Observations were carried out using confocal microscopy at 20x magnification. Phase photos at 10x magnification were taken for each condition to confirm the presence of the cell monolayer. **b** Endoglin fluorescence intensity following ECFC treatment with increasing concentrations of Thr-H (0.01, 0.1 and 1 μM) was quantified using ImageJ software ($n = 3$). **c** Plots showing the quantification of Eng fluorescence intensity in ECFC following treatment with 1 μM of Thr-H, alongside the number of nuclei relative to the surface. **d** Immunofluorescence staining of Eng using the Endoglin/CD105 P4A4-Alexa 488 antibody in different cell types, including HUVECs and MSCs, mounted with Vectashield containing DAPI. HUVECs were additionally stained with VE-Cadherin (VE-CAD) using a Texas Red-conjugated antibody, and MSCs were stained with Phalloidin-Alexa 555 to assess cell integrity after treatment with Thr. **e** Plots showing the quantification of Eng fluorescence intensity in HUVEC and MSC following treatment with 1 μM of Thr-H, alongside the number of nuclei relative to the surface. **f** ELISA kit assay results for sEng in supernatants of ECFC, HUVEC and MSC treated or not with 1 μM of Thr-H. The data is presented as mean ± S.D. for a minimum of $n = 4$. Statistical significance was considered at $^{*}P < 0.05$, $^{**}P < 0.01$, $^{***}P < 0.001$, and $^{****}P < 0.0001$.

underlying mechanisms and the functional effects[18]. When we performed in silico analysis of the Eng sequence we found a motif homologous to a Thr target peptide of PAR-1, a human receptor cleaved by Thr. PAR-1 is a heptahelical G protein-coupled receptor for Thr that is the prototype member of the PAR receptor family. Its activation occurs when Thr binds to and cleaves the N-terminal ectodomain of PAR-1 at a specific site. This cleavage results in the generation of a new N-terminus unmasking a "tethered ligand" that binds to the heptahelical segment of the receptor to effect transmembrane signaling and G protein activation[34]. Intriguingly, women with PE have been found to exhibit higher plasma tissue factor (TF) activity compared to those with small-for-gestational-age neonates or normal pregnancies[35,36]. TF is an integral membrane protein essential for hemostasis that circulates in blood either as a component of blood cells and microparticles or as a soluble plasma protein[36]. TF triggers the initiation of the coagulation cascade, resulting in the generation of Thr, which subsequently activates PAR-1. As a result, these alterations might partially contribute to the elevated in vivo Thr generation observed in this obstetrical syndrome[35]. Recent studies have also reported the involvement of plasma hypercoagulability, heightened Thr generation, compromised fibrinolysis, and endothelial cell activation in the development of severe preeclampsia[22]. These pieces of evidence led us to postulate that Thr cleaves Eng, and that the fragments produced are the ones postulated/found in preeclampsia plasma and serum. Firstly, we confirmed a statistically significant difference in terms of production of sEng between non-pregnant and pregnant women versus preeclampsia patients ($p < 0.0001$). Then, we identified different sizes of sEng at 60 kDa, 40 kDa and 20 kDa (Fig. 1, Supplementary Fig. 1). Before conducting in-vitro experiments, we developed an algorithm to predict possible Thr cleavages on Eng sequences. In silico predictions were made for potential cleavage sites, and some of the sites with the highest scores were subsequently confirmed to align with the observed cleavages in vitro following N-terminal and C-terminal sequencing assays.

Following the hypothesis suggested by in silico data, we were able to subsequently establish that Thr released Eng from cell surface across various cells including HUVECs, ECFCs and MSCs leading to the generation of sEng in the media (Fig. 5 and Supplementary Fig. 8). This previously unobserved cleavage event may offer an explanation not only for the existence of shorter endoglin fragments, as suggested by previous authors[7], but also for the presence of monomeric sEng[17]. This is attributable to two cleavage sites being situated upstream (R406/S407 and R510/A511) of the first intermolecular disulfide bridge (C516). We could therefore question why these different fragments were not identified in the past. If we examine literature, we find that the standard commonly used antibody to target Eng was P4A4, which is able to recognize only the sequence comprising I270-C330[37]. Importantly, we discovered that some of fragments originated by Eng cleavage are localized outside and downstream of the P4A4 recognition site. In fact, the 20 kDa band from S407 to G586, the 10 kDa band from A511 to G586 and the 8 kDa from S531 to G586 and they were identified using a Endoglin/CD105 polyclonal rabbit antibody (ProteinTech) that can recognize the C-terminal part of Eng sequence encoded by the 331–658 aa. This finding led us to hypothesize that the shorter fragments of Eng were not described before probably due to the fact that the previous antibodies used (P4A4 and MAB1097) recognized N-t sequences of the protein (Supplementary Fig. 2). Specifically P4A4 labeled only a small fragment from the aa 270 to 330 reducing the possibility to see fragments in plasma or serum[37]. In addition, the cleavages at S407, A511, S531 justify that after Thr cleavage, Eng loses C- disulphide bridges, still present in Eng and in sEng subjected only to MMP14 cleavage. This is in agreement with the presence of a monomeric form of Eng in plasma from PE patients[17,31]. These findings could have a physiological relevance because the production of different sEng lenghts depends on Thr production and might be a witness of a development or a worsening of the disease. Our results lead us to postulate that Thr can cut, either independently or simultaneously to MMPs, Eng or sEng during inflammation or at sites of dysfunctional endothelium. The fact that Thr targets Eng in multiple cleavages is likely at the origin of the different lengths of sEng found in PE plasma and serum and led us to propose sEng as a surrogate biomarker for the evaluation of the risk for severe early onset preeclampsia.

Materials and methods

Patient plasmas

In this study, we used samples from three groups of patients: pregnant women with PE, normotensive pregnant women without PE and healthy non pregnant women. The patients were recruited in 2 studies. Pregnant women with PE or without PE were enrolled in the ECLAXIR study[38], which is a multicenter case-control study (research grant from the regional *Programme Hospitalier de Recherche Clinique* P020925). The cases were pregnant women with PE at time of diagnosis, PE being defined according to the definition of the American College of Obstetricians and Gynecologists (ACOG) as blood pressure >140/90 mm Hg occurring after 20 weeks of gestation with previously normal blood pressure, associated with proteinuria >0.3 g in a 24 h urine specimen. The controls were pregnant normotensive women without PE. The ECLAXIR study was approved by the Ethics Committee (*Comité de Protection des Personnes dans la Recherche Biomédicale, CCPPRB*) of the Bichat-Claude Bernard hospital (Paris). Non pregnant women were enrolled in the SERCOB study[39], which is a case-control study (research Grant CRC 10018 *Contrat de Recherche Clinique from Assistance Publique–Hôpitaux de Paris*, clinical trials NCT00632671), where the controls were healthy women with age ≥18 and ≤60 years old, a body mass index (BMI) > 18.5 and <25 kg/m^2 and without weight variation >5 kg in the last 3 months. The SERCOB study was approved by the ethics committee of Saint-Louis University Hospital, Paris (France) (Institutional Review Board). For both studies, all patients gave written informed consent before enrolment and blood sampling and all samples were stored at −80 °C until testing. sEng was quantified by quantikine ELISA immunoassay kit performed on plasma ($n = 20$) and serum ($n = 20$) samples.

All ethical regulations relevant to human research participants were followed.

Sequence alignment

Alignments of human endoglin sequence with those of ten other mammal species were done online using Clustal Omega (v1.2.4)[40]. This is a multiple sequence alignment program that uses seeded guide trees and Hidden Markov Model profile techniques to generate the alignment. The amino acid sequences of different mammal species were obtained from the UniProt/SwissProt database.

Algorithm of binding sequence prediction

Bioinformatic analysis in search of possible cleavage sites on the Eng sequence by Thr through a Profile Specific Scoring Matrix (PSSM) analysis was performed. In ref. 41 53 peptide sequences were reported to be substrates for Thr cleavage and aligned around a central arginine from position P3 to position P4'. This alignment constitutes the dataset to extract a profile characterizing the cleavage motif. In a PSSM a score is associated with the presence of a given amino acid at a specific position of the motif, generating a scoring matrix. In our case the matrix is of dimension 20 × 8, i.e. 20 amino acids times 8 positions in the motif. The score is calculated computing the probability of occurrence of each amino acid at a given position from the known sequence alignments, normalized by its relative abundance in nature. Based on this scoring matrix it is then possible to analyze a new sequence in search for subsequences of the size of the motif. For the new sequence a score is computed adding the values of the PSSM corresponding to the amino acids of the subsequence at the position in which they appear in the motif. In our case, we scanned the whole endoglin sequence and for each arginine we computed the score of motifs P3 to P4'.

Docking analysis

X-ray crystallographic information on the orphan region and the ZP module that constitute the structure of the ectodomain of sEng is available in the Protein Data Bank with accession numbers 5I04 (orphan region, 2.42 Å resolution), 5HZW (orphan region/BMP complex, 4.45 Å resolution) and 5HZV (ZP module, 2.7 Å resolution)[24]; based on these experimental structures, a model of BMP9 ligand-bound homodimeric Eng was suggested, where the molecule adopts a Y-shaped open conformation. A low resolution negative stain EM map of unbound endoglin also exist, suggesting that the free molecule can also exist in a more compact, closed form[42]. Given the only structure available at atomistic resolution is that of the open ENG, we performed docking analysis using this model which also has the advantage of allowing Thr to approach Eng at the various sites identified by sequence analysis. The Thr structure used for docking was extracted from the high-resolution complex of Thr with an extra-cellular fragment of PAR1 receptor (PDB id 3LU9), in which Thr is found in an activated form, as the one it sould adopt for cleavage. Rigid protein-protein docking was performed using the program ClusPro[43] searching for positions of interaction between the two molecules that optimizes physical interactions (electrostatic interactions, hydrogen bonds, Van der Waals interactions). Because of the large size of the proteins and the fact that the possible binding sites on Eng identified by sequence analysis are at multiple distant regions, rigid docking seemed an appropriate compromise between accuracy and speed of the search[24,44]. All figures to illustrate docking results were produced using the Chimera software[45].

Recombinant endoglin (rEng) and thrombin

Recombinant endoglin (rEng), corresponding to human sEng containing the entire extracellular region (Glu26-Gly586), was obtained from R&D Systems (1097-EN-025/CF). Recombinant mouse Endoglin/CD105 Fc Chimera Protein, encompassing the extracellular region (Glu27-Gly581), was purchased from R&D Systems (1320-EN/CF). rEng (20 µg/mL) was diluted in Tris-buffered saline polyethylene glycol 1x buffer (TBS-PEG) and treated with human α-thrombin (Thr-H) (Cryopep, 9-HCT-0020-1) or human β-thrombin (Thr-C) (Cambridge ProteinWorks, #10108). Dose responses were performed with Thr-H from 0.01 to 1 µM for 1 h at 37 °C and kinetic with 1 µM of Thr-H during 1, 5, 15, 30 and 60 min at 37 °C. Reaction was stopped by adding 50 µM of Phe-Pro-Arg-chloromethylketone, an irreversible thrombin inhibitor (PPACK, Merck, 520222-5MG). Samples were then analysed by different methodologies.

Western blot and blue Coomassie staining

Samples (Thr-treated rEng, plasma and serum) were homogenized in an appropriate volume of 1x NuPAGE LDS Sample Buffer (Invitrogen, NP0007) supplemented with 1x NuPAGE Reducing Agent (Invitrogen, NP0009). Samples were then heat-denatured for 5 min at 80 °C and loaded on a NuPAGE 4–12% Bis-Tris polyacrylamide gel (Invitrogen, NP0323BOX). After running, the gels were then either stained with Coomassie brilliant blue (InstantBlue, Abcam, ab119211), de-stained for 2 h in distilled water and scanned before protein spot excision for further sequencing or the gels were transferred to nitrocellulose membranes for western blotting (WB). The membranes were saturated with 5% BSA in TBS-Tween 1x and incubated overnight at 4 °C with endoglin polyclonal rabbit antibody (1/1000, ProteinTech, #10862-1-AP) or endoglin monoclonal mouse antibody (1/500, R&D, MAB1097). Membranes were washed in TBS-Tween 1x and incubated for 1 h at room temperature with a fluorescent-labeled secondary antibody, Dylight 800-conjugated secondary antibody (1/10000, Thermo Fisher Scientific, SA5-10036). Fluorescent immunoblot images were acquired using an Odyssey scanner (Li-Cor Biosciences, Lincoln, NE, USA) and quantified using ImageJ or Image Studio Lite (Li-Cor) software.

Capillary electrophoresis immunoassay

Recombinant endoglin cleavage products and cells supernatant (MSCs and HUVECs) were analyzed after treatment with 1 µM of Thr-H or Thr-C using a capillary electrophoretic based immunoassay (WES; ProteinSimple, San Jose, CA), following the manufacturer's instructions. Briefly, the WES measurement was performed using a 2–40 kDa separation module (8 × 13 mm capillary cartridge, ProteinSimple Co., SM-W009) and endoglin polyclonal rabbit antibody (1/100).

N-terminal amino acid sequence analysis

The spots of interest were excised and incubated in a buffer to extract the protein from the acrylamide gel. After overnight incubation under shaking, the solution was incubated on a ProSorb Filter (Applied Biosystems) to fix the protein on a PVDF disc. The N-terminal sequences of proteins were determined by introducing the PVDF disc into an Applied Biosystems 494 automated protein sequencer (Applied Biosystems). Runs of Edman degradation (15 cycles of pulsed-liquid chemistry) were carried out. The sequences obtained were matched to public protein sequence databases with PATTINPROT, a software developed at the Pôle Bio-Informatique Lyonnais (PBIL) in Lyon, France (http://npsa-pbil.ibcp.fr), and with MS-PATTERN on the protein prospector web site (http://prospector.ucsf.edu). For inconclusive searches, sequences were matched against microbial genomes at the NCBI using the more general tBLASTn algorithm.

C-terminal protein characterization by mass spectrometry

Gel bands of proteolytic fragments were cut and subjected to in-gel digestions with different endoproteases (Trypsin, Asp-N or chymotrypsin) before submission to mass spectrometry analysis. Peptides mixtures were analyzed by nanoLC–MSMS using a nanoElute liquid chromatography system (Bruker) coupled to a timsTOF Pro mass spectrometer (Bruker). Peptides were loaded with solvent A on a trap column (nanoEase C18, 100 Å, 5 µm, 180 µm × 20 mm) and separated on an Aurora analytical column (ION OPTIK, 25 cm × 75 µm, C18, 1.6 µm) with a gradient of 0–35% of solvent B for 30 min. Solvent A was 0.1% formic acid and 2% acetonitrile in water and solvent B was acetonitrile with 0.1% formic acid. MS and MS/MS spectra were recorded from m/z 100 to 1700 with a mobility scan range from 0.6 to 1.4 V s/cm^2. MS/MS spectra were acquired with the PASEF (Parallel Accumulation Serial Fragmentation) ion mobility-based acquisition mode using a number of PASEF MS/MS scans set as 10. MS and MSMS raw data were processed and converted into mgf files with DataAnalysis software (Bruker). Identification and C-terminal characterization of protein were performed using the MASCOT search engine (Matrix Science, London, UK) with semi-specific cleavages against endoglin sequence. Carbamidomethylation of cysteines was set as fixed modification and oxidation of methionines as variable modification. Peptide and fragment tolerances were set at 10 ppm and 0.05 Da, respectively.

Cell isolation, culture and thrombin treatment

Endothelial Colony Forming Cells (ECFCs) were isolated as described[46], expanded on fibronectin (FN)-coated plates (1 µg/cm^2; Millipore, Billerica,

MA, USA) using EGM-2 medium (without hydrocortisone; Lonza, Walkersville, MD, USA) supplemented with 10% fetal bovine serum (FBS; Hyclone, Logan, UT, USA). Pooled Human Umbilical Vein Endothelial Cells (HUVECs) were purchased from Lonza (C-2519A) and seeded in a complete culture medium as described above for ECFCs. Mesenchymal Stem Cells (MSCs) were purchased from Lonza (PT-2501) and seeded in minimum essential medium α (MEM α) with GlutaMAX™ supplement, no nucleosides medium (Life Technologies, Gibco™, 32561094) supplemented with 10% of FBS (Dutscher, S1810-500), 10 ng/mL of fibroblast growth factor (FGF, R&D Systems®, 233-FB-500), and 1% of antibiotic/antimycotic (Thermo Fisher Scientific, Gibco™, 15240062). ECFCs, HUVECs, and MSCs were used at passages P2-8 and day <40. All cells were cultured in appropriate basal medium (controls) *vs* basal medium with Thr-H (concentrations 0.01, 0.1 and 1 µM, treatment 1 h at 37 °C). We consider for the study $n = 6$ ECFC (± Thr-H), $n = 4$ HUVEC (± Thr-H) cultured in EBM-2 and $n = 8$ MSC (± Thr-H) cultured in basal MEMα. Supernatant was recollected to perform ELISA assays, while cells were fixed with 4% paraformaldehyde (PFA) in PBS for 15 min at room temperature (RT) to perform immunofluorescence assays.

Quantitative assay of human endoglin by ELISA

Quantitative analysis of sEng in cell supernatants, as well as in plasma and serum samples was carried out via the sandwich enzyme-linked immunosorbent assay (ELISA) principle. Human Endoglin/CD105 quantikine ELISA immunoassay 96-well kits (R&D Systems, USA, MNDG00) were used according to the manufacturer's instructions. The ensuing product of the sandwich was read spectrophotometrically at 450 nm using a Spectrostar Nano-96 micro-well reader (BMG-Labteck).

Immunofluorescence

Cells incubated with or without Thr-H during 1 h were fixed with 4% PFA in medium for 15 min at room temperature (RT). Cells were then washed with Dulbecco's phosphate buffered saline (DPBS, ThermoFischer) and blocked in 2% BSA in PBS for 30 min at RT, incubated for 1 h at RT under agitation with Endoglin/P4A4 monoclonal mouse antibody (1/500, Santa Cruz, sc-20072) or VE cadherin (1/100 abcam) or Alexa Fluor 555 Phalloidin (1/200 ThermoFicher). Cells were then washed three times with PBS and then incubated with an anti-mouse fluorescein or Texsas Red-labeled secondary antibody (1/200, Vector Laboratories, FI-2000-1.5 and TI-1000 respectively) for 1 h at RT under agitation. Cells were washed three times with PBS, and the vectashield mounting medium for fluorescence with DAPI (1 mg/mL, Vector Laboratories, H-1200) was used. Cover slips were mounted onto slides that were stocked at 4 °C. Observations were performed on confocal microscopy at 20x (Confocal Laser Scanning Microscope, CLSM, Leica TCS SP5).

Statistics and reproducibility

Data were subjected to statistical analysis, and the results are shown as mean ± SD. Normality was analyzed with the Shapiro-Wilk test. When the test did not indicate normality, we performed a nonparametric analysis using the Mann-Whitney test. Otherwise, 2-group comparison was performed with parametric Student's *t*-test (unpaired).

Reporting summary

Further information on research design is available in the Nature Portfolio Reporting Summary linked to this article.

Data availability

The numerical source data underlying the graphs shown in the manuscript are provided in Supplementary Data 1. All other data supporting the findings of this study are available within the paper and its supplementary information files.

Received: 26 April 2024; Accepted: 15 February 2025;
Published online: 26 February 2025

References

1. López-Novoa, J. M. & Bernabeu, C. The physiological role of endoglin in the cardiovascular system. *Am. J. Physiol. Heart Circ. Physiol.* **299**, H959–H974 (2010).
2. Rossi, E., Bernabeu, C. & Smadja, D. M. Endoglin as an Adhesion Molecule in Mature and Progenitor Endothelial Cells: A Function Beyond TGF-β. *Front. Med. (Lausanne)* **6**, 10 (2019).
3. Rossi, E. et al. Co-injection of mesenchymal stem cells with endothelial progenitor cells accelerates muscle recovery in hind limb ischemia through an endoglin-dependent mechanism. *Thromb. Haemost.* **117**, 1908–1918 (2017).
4. Shovlin, C. L. Hereditary haemorrhagic telangiectasia: Pathophysiology, diagnosis and treatment. *Blood Rev.* **24**, 203–219 (2010).
5. Rossi, E., Lopez-Novoa, J. M. & Bernabeu, C. Endoglin involvement in integrin-mediated cell adhesion as a putative pathogenic mechanism in hereditary hemorrhagic telangiectasia type 1 (HHT1). *Front. Genet.* **5**, 457 (2014).
6. Puerto-Camacho, P. et al. Endoglin and MMP14 Contribute to Ewing Sarcoma Spreading by Modulation of Cell-Matrix Interactions. *Int J. Mol. Sci.* **23**, 8657 (2022).
7. Gregory, A. L., Xu, G., Sotov, V. & Letarte, M. Review: the enigmatic role of endoglin in the placenta. *Placenta* **35**, S93–S99 (2014).
8. Gougos, A. & Letarte, M. Primary structure of endoglin, an RGD-containing glycoprotein of human endothelial cells. *J. Biol. Chem.* **265**, 8361–8364 (1990).
9. Castonguay, R. et al. Soluble endoglin specifically binds bone morphogenetic proteins 9 and 10 via its orphan domain, inhibits blood vessel formation, and suppresses tumor growth. *J. Biol. Chem.* **286**, 30034–30046 (2011).
10. Jovine, L., Darie, C. C., Litscher, E. S. & Wassarman, P. M. Zona pellucida domain proteins. *Annu Rev. Biochem* **74**, 83–114 (2005).
11. Rossi, E. & Bernabeu, C. Novel vascular roles of human endoglin in pathophysiology. *J. Thromb. Haemost.* **21**, 2327–2338 (2023).
12. Bernabeu, C., Lopez-Novoa, J. M. & Quintanilla, M. The emerging role of TGF-beta superfamily coreceptors in cancer. *Biochim Biophys. Acta* **1792**, 954–973 (2009).
13. Vicen, M. et al. Membrane and soluble endoglin role in cardiovascular and metabolic disorders related to metabolic syndrome. *Cell Mol. Life Sci.* **78**, 2405–2418 (2021).
14. Gallardo-Vara, E. et al. Transcription factor KLF6 upregulates expression of metalloprotease MMP14 and subsequent release of soluble endoglin during vascular injury. *Angiogenesis* **19**, 155–171 (2016).
15. Hawinkels, L. J. A. C. et al. Matrix metalloproteinase-14 (MT1-MMP)-mediated endoglin shedding inhibits tumor angiogenesis. *Cancer Res.* **70**, 4141–4150 (2010).
16. Venkatesha, S. et al. Soluble endoglin contributes to the pathogenesis of preeclampsia. *Nat. Med.* **12**, 642–649 (2006).
17. Lawera, A. et al. Role of soluble endoglin in BMP9 signaling. *Proc. Natl. Acad. Sci. USA* **116**, 17800–17808 (2019).
18. Tang, H., Low, B., Rutherford, S. A. & Hao, Q. Thrombin induces endocytosis of endoglin and type-II TGF-beta receptor and down-regulation of TGF-beta signaling in endothelial cells. *Blood* **105**, 1977–1985 (2005).
19. Esmon, C. T. The protein C pathway. *Chest* **124**, 26S–32S (2003).
20. Vergnolle, N., Derian, C. K., D'Andrea, M. R., Steinhoff, M. & Andrade-Gordon, P. Characterization of thrombin-induced leukocyte rolling and adherence: a potential proinflammatory role for proteinase-activated receptor-4. *J. Immunol.* **169**, 1467–1473 (2002).
21. Erez, O. et al. Perturbations in kinetics of the thrombin generation assay identify women at risk of preeclampsia in the first trimester and provide the rationale for a preventive approach. *Am. J. Obstet. Gynecol.* **228**, 580.e1–580.e17 (2023).
22. Van Dreden, P. et al. The procoagulant phospholipid dependent clotting time and the initiation phase of thrombin generation test are

mandatory for the evaluation of the risk for severe early onset preeclampsia. *Thromb. Res.* **217**, 57–59 (2022).
23. Gieseler, F., Ungefroren, H., Settmacher, U., Hollenberg, M. & Kaufmann, R. Proteinase-activated receptors (PARs)—Focus on receptor-receptor-interactions and their physiological and pathophysiological impact. *Cell Commun. Signal.: CCS* **11**, 86 (2013).
24. Saito, T. et al. Structural Basis of the Human Endoglin-BMP9 Interaction: Insights into BMP Signaling and HHT1. *Cell Rep.* **19**, 1917–1928 (2017).
25. García, P. S. et al. Concentration-Dependent Dual Role of Thrombin in Protection of Cultured Rat Cortical Neurons. *Neurochem Res.* **40**, 2220–2229 (2015).
26. Allen, G. A. et al. Impact of procoagulant concentration on rate, peak and total thrombin generation in a model system. *J. Thromb. Haemost.* **2**, 402–413 (2004).
27. Krenzlin, H. et al. High CSF thrombin concentration and activity is associated with an unfavorable outcome in patients with intracerebral hemorrhage. *PLoS ONE* **15**, e0241565 (2020).
28. Rossi, E. et al. Endoglin regulates mural cell adhesion in the circulatory system. *Cell Mol. Life Sci.* **73**, 1715–1739 (2016).
29. Schmella, M. J. et al. Plasma concentrations of soluble endoglin in the maternal circulation are associated with maternal vascular malperfusion lesions in the placenta of women with preeclampsia. *Placenta* **78**, 29–35 (2019).
30. Valbuena-Diez, A. C. et al. Oxysterol-induced soluble endoglin release and its involvement in hypertension. *Circulation* **126**, 2612–2624 (2012).
31. Andersson-Rusch, C. et al. High concentrations of soluble endoglin can inhibit BMP9 signaling in non-endothelial cells. *Sci. Rep.* **13**, 6639 (2023).
32. Kaitu'u-Lino, T. J., Palmer, K., Tuohey, L., Ye, L. & Tong, S. MMP-15 is upregulated in preeclampsia, but does not cleave endoglin to produce soluble endoglin. *PLoS ONE* **7**, e39864 (2012).
33. Kaitu'u-Lino, T. J. et al. MT-MMPs in pre-eclamptic placenta: relationship to soluble endoglin production. *Placenta* **34**, 168–173 (2013).
34. Ludeman, M. J. et al. PAR1 Cleavage and Signaling in Response to Activated Protein C and Thrombin. *J. Biol. Chem.* **280**, 13122–13128 (2005).
35. Erez, O. et al. Tissue Factor Activity in Women with Preeclampsia or SGA: A Potential Explanation for the Excessive Thrombin Generation in These Syndromes. *J. Matern Fetal Neonatal Med.* **31**, 1568–1577 (2018).
36. Butenas, S., Bouchard, B. A., Brummel-Ziedins, K. E., Parhami-Seren, B. & Mann, K. G. Tissue factor activity in whole blood. *Blood* **105**, 2764–2770 (2005).
37. Pichuantes, S. et al. Mapping epitopes to distinct regions of the extracellular domain of endoglin using bacterially expressed recombinant fragments. *Tissue Antigens* **50**, 265–276 (1997).
38. Stepanian, A. et al. Search for an association between V249I and T280M CX3CR1 genetic polymorphisms, endothelial injury and preeclampsia: the ECLAXIR study. *PLoS ONE* **4**, e6192 (2009).
39. Elaïb, Z. et al. Platelet Functions are Decreased in Obesity and Restored after Weight Loss: Evidence for a Role of the SERCA3-Dependent ADP Secretion Pathway. *Thromb. Haemost.* **119**, 384–396 (2019).
40. Sievers, F. et al. Fast, scalable generation of high-quality protein multiple sequence alignments using Clustal Omega. *Mol. Syst. Biol.* **7**, 539 (2011).
41. Gallwitz, M., Enoksson, M., Thorpe, M. & Hellman, L. The extended cleavage specificity of human thrombin. *PLoS ONE* **7**, e31756 (2012).
42. Llorca, O., Trujillo, A., Blanco, F. J. & Bernabeu, C. Structural model of human endoglin, a transmembrane receptor responsible for hereditary hemorrhagic telangiectasia. *J. Mol. Biol.* **365**, 694–705 (2007).
43. Kozakov, D. et al. The ClusPro web server for protein-protein docking. *Nat. Protoc.* **12**, 255–278 (2017).
44. Desta, I. T., Porter, K. A., Xia, B., Kozakov, D. & Vajda, S. Performance and Its Limits in Rigid Body Protein-Protein Docking. *Structure* **28**, 1071–1081.e3 (2020).
45. Pettersen, E. F. et al. UCSF Chimera–a visualization system for exploratory research and analysis. *J. Comput Chem.* **25**, 1605–1612 (2004).
46. Smadja, D. M. et al. Bone Morphogenetic Proteins 2 and 4 Are Selectively Expressed by Late Outgrowth Endothelial Progenitor Cells and Promote Neoangiogenesis. *Arterioscler Thromb. Vasc. Biol.* **28**, 2137–2143 (2008).

Acknowledgements

"This Manuscript is in honneur of Dr Bernard Le Bonniec, DR-Inserm UMR_S1140. Dr Le Bonniec dedicated his life to research and was the first to believe in this project. Unfortunately he left us on 23th December 2022".The authors thank Florence Sensi (UMRS1140) for managing E. Rossi's grants; the Medicine, Toxicology, Chemistry, Imaging doctoral school (MTCI ED 563) for D. El Hamaoui (PhD student of E. Rossi) salary; Laurant Coquet - Plateforme de Proteomique PISSARO – UMR6270 CNRS, Université de Rouen, Normandie for N-Ter Edman sequencing; David Cornu Plateforme de Proteomique Gif-sur-Yvette, Université Paris-Saclay. We thank the "Cellular and Molecular Imaging Facility", US25 Inserm, UAR3612 CNRS, Faculty of Pharmacy, Université Paris Cité (4, avenue de l'Observatoire, F-75006 Paris, France) for technical support. L. Jovine was supported by the Knut and Alice Wallenberg Foundation (grant 2018.0042) and the Swedish Research Council (grant 2020-04936).

Author contributions

E. Rossi. designed and supervised the research, analyzed the data, wrote the paper and provide financial aid; D. El Hamaoui performed the assays, discussed results and wrote part of material and methods. A. Marchelli and B. Palmier performed some assays. A. Kauskot discussed results, performed assays and participated to writing the manuscript. S. Pasquali and E. Reboul performed computational analysis and docking. L. Jovine provided the model of homodimeric endoglin and was involved in the discussion of structural aspects. A. Stepanian provided plasma and serum of patients. S. Gandrille performed sequence alignments and the analysis of glycosylation. P. Gaussem, D. Smadja, C. Denis, C. Bernabeu and F. Lebrin provided helpful advices for improving the article.

Competing interests

A patent (No. EP24307100) entitled 'Peptide derived from endoglin for treating bleeding disorders' was filed by inventor Elisa Rossi and supported by INSERM Transfert (Institut National de la Santé et de la Recherche Médicale) in France.

Additional information

Supplementary information The online version contains supplementary material available at https://doi.org/10.1038/s42003-025-07751-3.

Correspondence and requests for materials should be addressed to Elisa Rossi.

Peer review information *Communications Biology* thanks the anonymous reviewers for their contribution to the peer review of this work. Primary Handling Editors: Toril Holien and Dario Ummarino.